Journal of Green Energy Research and Innovation

Adaptive Backstepping Control of an Autonomous Multi-Bus Microgrid based on Grid-forming/Grid-following Strategy Under Unbalanced Load Conditions

Mohammad Mahdi Rezaei

Highlights

- **Microgrid Control: A robust strategy maintains voltage and frequency in multi-bus island microgrids.**
- **Grid-forming/Grid-following: Adaptive backstepping controls voltage and frequency, while direct power control manages active/reactive powers.**
- **Local Measurement-based Design: The system uses local measurements for control, independent of microgrid specifics.**
- **Stability and Robustness: The controllers ensure stable operation, handling disturbances and parameter uncertainties effectively.**

Graphical Abstract

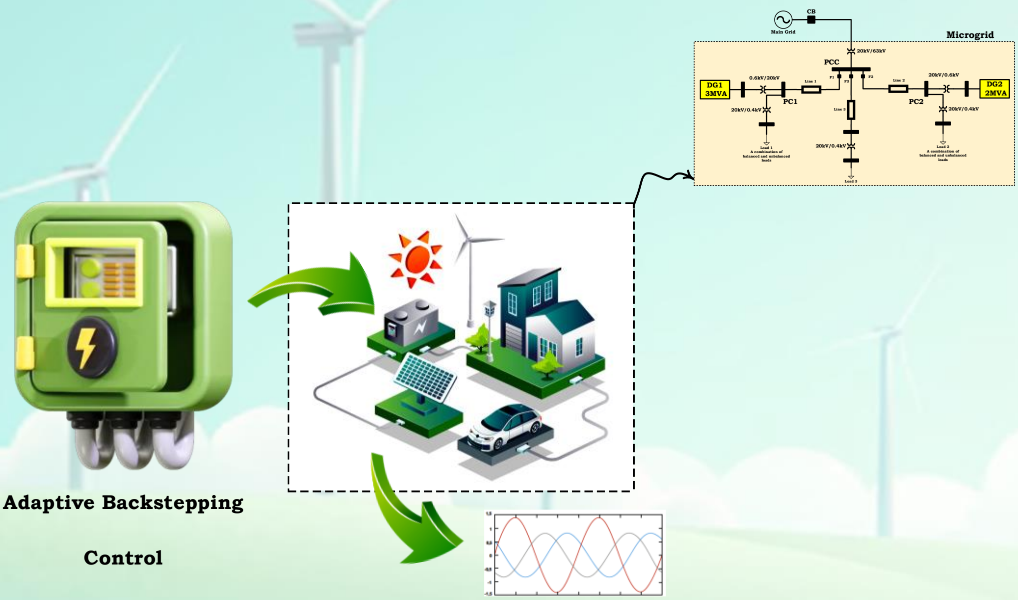

Use your device to scan and read the article online

Citation
M.M. Rezaie," Adaptive Backstepping Control of an Autonomous Multi-Bus Microgrid based on Grid-forming/Grid-following Strategy Under Unbalanced Load Conditions," *Journal of Green Energy Research and Innovation*, vol. 2, no. 1, pp. 20-31, 2025.

https://doi.org/10.61186/jgeri.2.1.20

JGERI Journal of Green Energy Research and Innovation

Journal of Green Energy Research and Innovation 2.1 (2025) 20-31

Online ISSN: 3041-9018

Journal of Green Energy Research and Innovation

Journal Homepage: www.jgeri.araku.ac.ir

Adaptive Backstepping Control of an Autonomous Multi-Bus Microgrid based on Grid-forming/Grid-following Strategy Under Unbalanced Load Conditions

Mohammad Mahdi Rezaei [*]

Department of Electrical Engineering, Khomeinishahr Branch, Islamic Azad University, Khomeinishahr, Isfahan, Iran.

A R T I C L E I N F O

Keywords:
Microgrid (MG),
Distributed Generation (DG),
Grid-forming/Grid-following control structure,
Adaptive Backstepping.

Article History:
Received: 26 June 2024;
Revised: 19 July 2024;
Accepted: 11 August 2024.

Article type:
Research Article

* ***Corresponding author***
E-mail address:
mm.rezaei@iaukhsh.ac.ir (M. Rezaie)

A B S T R A C T

In this article, in order to maintain the voltage and frequency of a multi-bus island microgrid, a robust control strategy is proposed. The microgrid under study is a medium voltage distribution system consisting of several inverter-based distributed generation (DG) units, and a combination of balanced and unbalanced local loads. Based on the Grid- forming/Grid-following structure, a robust voltage controller is designed based on the adaptive backstepping control method to keep the voltage and frequency of the Grid-forming unit at predefined values. In addition, to adjust the active/reactive powers of the Grid-following units, a direct power controller based on adaptive input-output feedback linearization control method is proposed. The negative sequence component of unbalanced local loads current is compensated by the proposed power controller. Only local measurements are used in designing of the controllers; therefore, the proposed method is independent of the topology of microgrid, the parameters of the system, and the dynamics of loads. The controllers presented in this article are robust and stable against various disturbances and parameter uncertainties. after outage of Grid-following unit, the power generated by the Grid-forming unit is adaptively adjusted so that the absence of generation at PC2 is offset. In addition, despite the mismatched filter resistance and accidental outage of Grid-following unit, even under non-local unbalanced load condition the proposed voltage controller robustly regulates the voltage waveform of MG with a reasonable transient. Validity and effectiveness of the proposed control strategy are shown based on time domain studies in MATLAB/Simulink environment.

1. Introduction

1.1. Problem statement

Microgrids (MGs) are low- or medium-voltage local networks that include clusters of loads as well as distributed generation (DG) units [1-5]. Depending on the conditions, MGs can be operated both in grid connected mode and in islanded mode. In the mode of connected to the grid, the voltage of the buses and the frequency of the system are dictated by the main grid, and each DG unit generates predetermined values of active/reactive power [6-7]. Considering MG's performance as an independent system in islanded mode, it is necessary to perform a proper voltage and frequency control. To enhance the reliability of the MG, this process should be performed robust, fast, and locally [8-9].

1.2. Literature Review

Several methods have been presented so far for the voltage/frequency control of islanded MGs [3-15, 19-25]. The main control strategies reported so far are methods based on Droop characteristic, and methods based on Grid-forming/Grid-following control structure [10]. Droop characteristic technique is the most well-known control strategy for MGs [3-15]. All DG units, in the methods based on Droop characteristic, participate in the voltage/frequency regulation of MG [11]. In this method, the total active/reactive power demand is shared locally among the DG units without using any MG communication. However, MG voltage and frequency deviations are unavoidable in this method [12]. In Grid-forming/Grid-following methods, the task of voltage and frequency regulation in MG is assigned to a DG unit, which usually has the highest power rating [14]. The name of this unit is called Grid-forming. Other units in MG, which are called Grid-following units, are responsible for generating predetermined active/reactive power.

Through appropriate control strategies, in addition to the main control purpose, the power quality of system can also be enhanced [15]. Voltage imbalance is the most common phenomenon among various power quality issues. Connection of unbalanced loads is the main cause of voltage unbalance in MGs. In actual distribution systems, due to the installation of a large number of unbalanced loads in different phases, the severity of overall load imbalance is not significant [16]. However, in MG systems, the problem of unbalanced loads is much more common and is caused by the unequal connection of unbalanced loads to the phases [17]. So, MGs are expected to be operated in such a way that they can perform properly even under unbalanced load conditions [18].

Therefore, both in the Droop and Grid-forming/Grid-following methods, to improve the dynamic behavior and achieve a disturbance rejection performance, the control scheme should be robust and fast in the island MG [19,23]. In the technical literature, various techniques have been reported for strong control of island MGs [19-24]. In [19], to improve the performance of MG, a changeable control structure in integration with the Droop characteristic technique is presented. A hierarchical two-stage control method is used in [20], which provides a centralized control strategy based on the cluster-oriented cooperative control strategy. By using this controller, it has been tried to optimize the sharing performance of power components in a multiple-MG system. However, the local controllers provided at the primary control level are based on the traditional droop method. In [21,22], the load dynamics is modeled with an RLC network and used in controller design process to achieve a suitable dynamic in the MG. Nevertheless, the stability and robustness of presented controllers cannot be cannot guaranteed against uncertainties in load configuration and dynamics.

In [23], a robust controller is proposed based on H_∞ control technique, to voltage/frequency control of a single-bus elementary MG. Using the Grid-forming/Grid-following structure, the load disturbance is measured in real-time and the Grid-forming unit's controller uses it as a measurable external disturbance. However, because of high-bandwidth communications needed between the Grid-forming unit and all further loads in multi-bus MGs, for real-time measurement of the instantaneous load currents, the presented scheme in [23] can be impractical. The Grid-following unit is connected to some load buses to participate the demand of load. Although it is explained in [23] that the Grid-following unit is operated based on vector control method, no description is presented in this case. Moreover, the Grid-following unit during load disturbances is disconnected and the performance of the Grid-following units has not been studied against load disturbances. In addition, there is no guarantee for the stability and effectiveness of the control structure due to the parametric uncertainties of the system.

In [24] a combination of proportional-integrating-based (PI) and proportional-resonance-based (PR) methods are used to respectively control of the positive-sequence (PS) voltage and compensate the negative-sequence (NS) current components. Two equivalent circuits are presented in [24] for PS and NS load currents. However, since both the PS and NS voltages are linear functions of both the PS and NS currents, the presented equivalent circuits are coupled and cannot be used separately. In [25], a robust control strategy is presented for a multi-bus MG. In the control system presented in [25], the voltage regulation of MG is fulfilled by a sliding-mode voltage controller for the Grid-forming unit. However, the power controller designed for the Grid-following unit only regulates its own output power and does not play a role in compensating the effects of the imbalance of its local loads. This causes all the burden of load imbalance compensation to fall on the Grid-forming unit.

1.3. Research gap

According to the conducted research, we realize that none of them used the adaptive backstepping control method to control the network. Also, few articles have designed their proposed controller based on unbalanced load control.

1.4. Main contribution and innovations

The main contribution of this paper is to propose a robust voltage controller, based on adaptive backstepping control method, to force the voltage and frequency of the Grid-forming unit to track the relevant references, in the Grid-forming/Grid-following control structure of a multi-island MGs.

In addition, a direct power controller is proposed based on adaptive input-output feedback linearization (IOFL) for the Grid-following units, to control the PS active/reactive powers generated by these units. The presented power controller is designed to be able to compensate the NS current components (NSCCs) caused by unbalanced local loads. The presented control strategy is based on local measurements and is independent of topology, parameters and dynamics of microgrid loads. Performance of the presented control system have been shown through simulation studies in the MATLAB/Simulink.

2. Microgrid Structure Description

Figure 1 shows the single-line diagram of the studied MG, including three radial feeders [24-25]. MG is fed by two 0.6 kV DG units with capacity of 3 MVA (DG1) and 2 MVA (DG2), respectively. The DG units are modeled with a DC source that connected to medium voltage (MV) feeders through a power converter, an LC filter, and step-up transformers. A combination of balanced and unbalanced loads is also connected to MV feeders F1, F2 and F3 through step-down transformers. In this paper, MG operates in island mode. Table 1 shows the parameters of MG.

3. DG Unit Modeling

Figure 2(a) depicts an inverter-based DG unit connected to a microgrid interface through an LC filter. Taking into account the parameters under nominal conditions, the dynamic Equation (1,2) of output voltage and current can be derived in the synchronous (dq) reference frame, as shown in Figure 2(b).

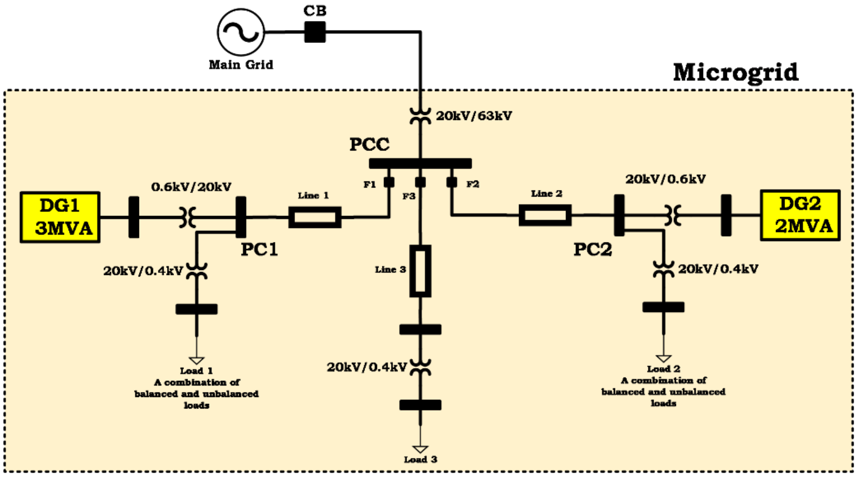

Figure 1. Schematic diagram of studied MG.

Table 1. Parameters of the studied system.

Parameter	Value
Grid-forming DG nominal power	3 MVA (S_{base})
Grid-following DG nominal power	2 MVA
VSC terminal voltage (line to line)	600 V (V_{base})
R_{f1}, R_{f2} (Series filter resistance)	0.002 Ω
L_{f1}, L_{f2} (Series filter inductance)	500 µH
C_{f1}, C_{f2} (Filter capacitance)	400 µF
Z_{line1} (5.7 km overhead line)	0.7 + j1.57 Ω
Z_{line2} (4 km overhead line)	0.5 + j1.25 Ω
Z_{line3} (2 km overhead line)	0.1 + j0 Ω
V_{dc} (DC bus voltage)	1500 V
f_S (System frequency)	50 Hz
f_{SW} (Switching frequency)	2 kHz

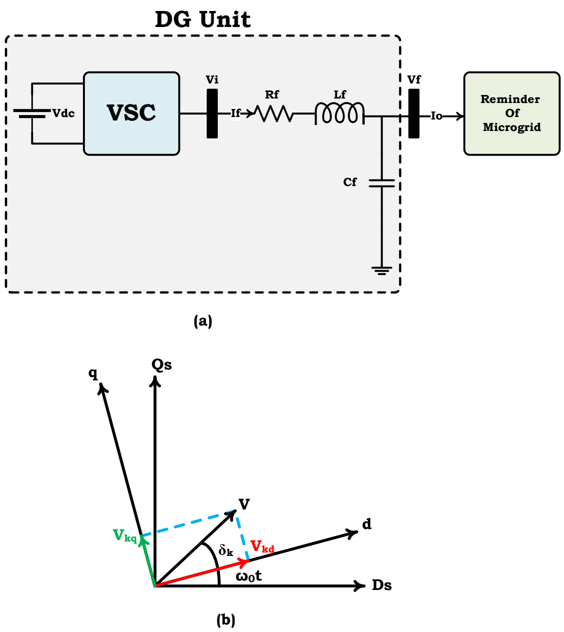

Figure 2. (a) Schematic diagram of a DG unit, (b) virtual synchronous reference frame.

$$\frac{d}{dt}I_f = a\left(V_i - bI_f - V_f\right) + \omega_0 I_f^{\perp}, \quad (1)$$

$$\frac{d}{dt}V_f = c\left(I_f - I_o\right) + \omega_0 V_f^{\perp}, \quad (2)$$

where the values of $a = \frac{1}{L_f}$, $b = R_f$ and $c = \frac{1}{C_f}$ represent the parameters in nominal conditions; the symbols in bold denote $V = [V_d V_q]^T$ and $I = [I_d I_q]^T$. Additionally, the superscript " $\perp$ " indicates a 90° lag with respect to the original vector. By deviating the system's parameters with respect to nominal values, Equations (1,2) can be rewritten as Equations (3,4):

$$\frac{d}{dt}\mathrm{I}_f = a\left(\mathrm{V}_i - b\mathrm{I}_f - \mathrm{V}_f\right) + \omega_0 \mathrm{I}_f^{\perp} + \Theta_i, \quad (3)$$

$$\frac{d}{dt}\mathrm{V}_f = c\left(\mathrm{I}_f - \mathrm{I}_o\right) + \omega_0 \mathrm{V}_f^{\perp} + \Theta_v, \quad (4)$$

The lumped uncertainties, denoted as $\Theta_i = [\Theta_{id}\Theta_{iq}]^T$ and $\Theta_v = [\Theta_{vd}\Theta_{vq}]^T$, can be expressed as Equations (5,6):

$$\Theta_i = \Delta a\left(\mathrm{V}_i - b\mathrm{I}_f - \mathrm{V}_f\right) - (a + \Delta a)\Delta b\mathrm{I}_f + \Lambda_i, \quad (5)$$

$$\Theta_v = \Delta c\left(\mathrm{I}_f - \mathrm{I}_o\right) + \Lambda_v, \quad (6)$$

where Δ denotes deviation from the expected value. In Equations (5,6), the terms Λ_i and Λ_v are introduced to address system dynamic disturbances and other unmodeled uncertainties.

4. Control Scheme

Based on Grid-forming/Grid-following control strategy in the context of a MG, DG_1 is specifically assigned the task of voltage control as a Grid-forming unit, and DG_2 has the specific role of generating predetermined levels of both active/reactive power components, as a Grid-following unit. In order to improve transient response and achieve desirable disturbance rejection and reference tracking performance, a robust voltage controller is specifically developed based on adaptive Backstepping for the Grid-forming unit. Additionally, a direct power controller has been developed based on adaptive IOFL. This controller ensures robust regulation of both active/reactive power levels that need to be supplied by Grid-following unit. In the subsequent subsections, a detailed explanation of the control design procedure is provided.

4.1. Adaptive Backstepping Control of Grid-forming Unit

The primary control objective for the Grid-forming (DG1) unit is to accurately follow the predefined voltage trajectories. Let's denote the voltage tracking error as Equation (7):

$$\mathrm{E}_v = \mathrm{V}_f^{ref} - \mathrm{V}_f, \quad (7)$$

and denote the error between the lumped uncertainties Θ_v and its estimated value $\hat{\Theta}_v$ as Equation (8):

$$\tilde{\Theta}_v = \hat{\Theta}_v - \Theta_v. \quad (8)$$

A Lyapunov function can be expressed as Equation (9):

$$W_1 = \frac{1}{2}\mathrm{E}_v^T\mathrm{E}_v + \frac{1}{2}\tilde{\Theta}_v^T\gamma_v\tilde{\Theta}_v, \quad (9)$$

where diagonal matrix γ_v consists of positive entries that are the estimation coefficients. Let's differentiate W_1 with respect to time as Equation (10):

$$\frac{d}{dt}W_1 = \mathrm{E}_v^T\left(\frac{d}{dt}\mathrm{E}_v\right) + \tilde{\Theta}_v^T\gamma_v\left(\frac{d}{dt}\tilde{\Theta}_v\right), \quad (10)$$

considering (7), (8) and (4), one can be shown as Equation (11):

$$\frac{d}{dt}W_1 = E_v^T\left(\frac{d}{dt}V_f^{ref} - c\left(I_f - I_o\right) - \omega_0 V_f^{\perp} - \Theta_v\right) + \tilde{\Theta}_v^T\gamma_v\left(\frac{d}{dt}\hat{\Theta}_v\right). \quad (11)$$

Choosing the estimation law as Equation (12):

$$\frac{d}{dt}\hat{\Theta}_v = -\gamma_v^{-1}E_v, \quad (12)$$

$\frac{d}{dt}W_1$ can be reduced to Equation (13):

$$\frac{d}{dt}W_1 = E_v^T\left(\frac{d}{dt}V_f^{ref} - c\left(I_f - I_o\right) - \omega_0 V_f^{\perp} - \hat{\Theta}_v\right). \quad (13)$$

For E_v to be stable, it is required that $\frac{d}{dt}W_1$ definitely be negative. By choosing Equation (14):

$$\mathrm{I}_f^{ref} = \mathrm{I}_o + \frac{1}{c}\left(\tfrac{d}{dt}\mathrm{V}_f^{ref} - \omega_0 \mathrm{V}_f^{\perp} - \hat{\Theta}_v + \mathrm{k}_v \mathrm{E}_v\right), \tag{14}$$

where diagonal matrix k_v consists of positive constant elements, then, it can be obtained as Equation (15):

$$\tfrac{d}{dt}W_1 = -\mathrm{k}_v \mathrm{E}_v^T \mathrm{E}_v + c\mathrm{E}_v^T \mathrm{E}_i \tag{15}$$

With Equation (16):

$$\mathrm{E}_i = \mathrm{I}_f^{ref} - \mathrm{I}_f \tag{16}$$

It can be concluded from Equation (15) that the system is not yet made fully stable. According to Backstepping control theory [26], the control input V_i should be designed in the next step to make $\frac{d}{dt}W_1$ negative definite. Hence, the following positive definite function can be chosen as Lyapunov function Equation (17):

$$W_2 = W_1 + \frac{1}{2}\mathrm{E}_i^T \mathrm{E}_i + \frac{1}{2}\tilde{\Theta}_i^T \gamma_i \tilde{\Theta}_i, \tag{17}$$

With Equation (18):

$$\tilde{\Theta}_i = \hat{\Theta}_i - \Theta_i, \tag{18}$$

where $\tilde{\Theta}_i$ is the error between lumped uncertainties Θ_i and its estimated value $\hat{\Theta}_i$. Time derivation of W_2 is obtained as Equation (19):

$$\frac{d}{dt}W_2 = \frac{d}{dt}W_1 + E_i^T\left\{\frac{d}{dt}E_i\right\} + \tilde{\Theta}_i^T \gamma_i \left(\frac{d}{dt}\tilde{\Theta}_i\right). \tag{19}$$

Considering (16), (18) and (3), it can be shown as Equation (20):

$$\frac{d}{dt}W_2 = -k_v E_v^T E_v + cE_v^T E_i + E_i^T\left\{\frac{d}{dt}I_f^{ref} - a\left(V_i - bI_f - V_f\right) - \omega_0 I_f^{\perp} - \Theta_i\right\} + \tilde{\Theta}_i^T \gamma_i \left(\frac{d}{dt}\hat{\Theta}_i\right). \tag{20}$$

If the estimation law is selected as Equation (21):

$$\tfrac{d}{dt}\hat{\Theta}_i = -\gamma_i^{-1}\mathrm{E}_i, \tag{21}$$

where γ_i is a diagonal matrix with positive constant elements, then $\frac{d}{dt}W_2$ becomes as Equation (22):

$$\frac{d}{dt}W_2 = -k_v E_v^T E_v + E_i^T\left\{cE_v + \frac{d}{dt}I_f^{ref} - a\left(V_i - bI_f - V_f\right) - \omega_0 I_f^{\perp} - \hat{\Theta}_i\right\}. \tag{22}$$

If the following control law is selected as Equation (23):

$$\mathrm{V}_i = \mathrm{V}_f + b\mathrm{I}_f + \frac{1}{a}\left(c\mathrm{E}_v + \tfrac{d}{dt}\mathrm{I}_f^{ref} - \omega_0 \mathrm{I}_f^{\perp} - \hat{\Theta}_i + \mathrm{k}_i \mathrm{E}_i\right) \tag{23}$$

where k_i is a diagonal matrix with positive constant elements, then $\frac{d}{dt}W_2$ can be obtained as Equation (24):

$$\frac{d}{dt}W_2 = -\mathrm{k}_v \mathrm{E}_v^T \mathrm{E}_v - \mathrm{k}_i \mathrm{E}_i^T \mathrm{E}_i \le 0. \tag{24}$$

It is shown that the time derivative of the Lyapunov function W_2 is strictly negative, therefore it implies that the proposed voltage control system is asymptotically stable.

4.2. IOFL Control of Grid-following DG Units

4.2.1. Power controller design

For Grid-following units, the primary control objective is to manage the active/reactive power supplied by the generation units. In the subsequent sections, it will delve into the detailed design procedure of the presented power controller. The instantaneous active/reactive power components produced by the DG unit can be mathematically represented as Equations (25,26) [28-29]:

$$P = \mathrm{V}_f \cdot \mathrm{I}_f = V_{fd} I_{fd} + V_{fq} I_{fq} \tag{25}$$

$$Q = \mathrm{V}_f^{\perp} . I_f = V_{fq} I_{fd} - V_{fd} I_{fq} \tag{26}$$

In Equations (25,26), the symbol " $\cdot$ " represents the inner product of two vectors, and the superscript " $\perp$ " indicates a phase lag of 90° with respect to the original vector. Based on Equations (25,26), the matrix form of instantaneous power equation of DG units can be expressed as Equation (27):

$$\mathrm{S} = \mathrm{E}_f \mathrm{I}_f \tag{27}$$

With Equation (28,29):

$$S = [P \quad Q]^T, \tag{28}$$

$$E_f = \begin{bmatrix} V_{fd} & V_{fq} \\ V_{fq} & -V_{fd} \end{bmatrix}. \tag{29}$$

By differentiating (27), it can be obtained that as Equation (30)

$$ddt\boldsymbol{S} = ddt\boldsymbol{E}f\, I_f + E_f\left(\frac{d}{dt} I_f\right) \tag{30}$$

If $\frac{d}{dt}V_{f,dq}$ and $\frac{d}{dt}I_{f,dq}$ are substituted into Equation (31), it can be expressed as Equation (31):

$$\frac{d}{dt}S = G + H + aE_f V_i + \Upsilon_s, \tag{31}$$

With Equation (32):

$$G = \begin{bmatrix} c\left(I_{fd} - I_{od}\right) + \omega_0 V_{fq} & c\left(I_{fq} - I_{oq}\right) - \omega_0 V_{fd} \\ c\left(I_{fq} - I_{oq}\right) - \omega_0 V_{fd} & -c\left(I_{fd} - I_{od}\right) - \omega_0 V_{fq} \end{bmatrix} I_f, \tag{32}$$

$$H = -E_f \begin{bmatrix} a\left(bI_{fd} + V_{fd}\right) - \omega_0 I_{fq} \\ a\left(bI_{fq} + V_{fq}\right) + \omega_0 I_{fd} \end{bmatrix}, \tag{33}$$

$$\Upsilon_s = \begin{bmatrix} \Theta_{vd} & \Theta_{vq} \\ \Theta_{vq} & -\Theta_{vd} \end{bmatrix} I_f + E_f \begin{bmatrix} \Theta_{id} & \Theta_{iq} \\ \Theta_{iq} & -\Theta_{id} \end{bmatrix}, \tag{34}$$

where the vector Υ_s represents the lumped uncertainties affecting the dynamics of S. Based on the IOFL control theory [27], by choosing the control input V_i as Equation (35):

$$\mathrm{V}_i = \tfrac{1}{a}\mathrm{U}_f^{-1}\left(-\mathrm{G} - \mathrm{H} + \mathrm{U}_i\right), \tag{35}$$

where U_i should be determined as a new control input, $\frac{d}{dt}\mathrm{S}$ can be expressed as Equation (36):

$$\tfrac{d}{dt}\mathrm{S} = \mathrm{U}_i + \mathrm{Y}_s \tag{36}$$

Letting the tracking error denoted by Equation (37):

$$\mathrm{E}_s = \mathrm{S}^{ref} - \mathrm{S}, \tag{37}$$

and the error between the lumped uncertainties Υ_s and its estimated value $\hat{\Upsilon}_s$ denoted by Equation (38):

$$\tilde{\Upsilon}_s = \hat{\Upsilon}_s - \Upsilon_s, \tag{38}$$

a positive definite Lyapunov function can be chosen as Equation (39):

$$W_3 = \frac{1}{2}E_s^T E_s + \frac{1}{2}\tilde{\Upsilon}_s^T \gamma_s \tilde{\Upsilon}_s, \tag{39}$$

where γ_s is a diagonal matrix with all positive constant diagonal entries which are the adaptation law gains. Differentiating W_3 with respect to time gives Equation (40):

$$\frac{d}{dt}W_3 = E_s^T\left(\frac{d}{dt}E_s\right) + \hat{\Upsilon}_s^T \gamma_s \left(\frac{d}{dt}\tilde{\Upsilon}_s\right). \tag{40}$$

By selecting the adaptation law as Equation (41):

$$\frac{d}{dt}\hat{\Upsilon}_s = -\gamma_s{}^{-1} E_s, \tag{41}$$

then, $\frac{d}{dt}W_3$ can be given by Equation (42):

$$\frac{d}{dt}W_3 = E_s^T\left(\frac{d}{dt}S^{ref} - U_i - \hat{\Upsilon}_s\right). \tag{42}$$

Now by choosing the control input U_i as Equation (43):

$$U_i = \frac{d}{dt}S^{ref} - \hat{\Upsilon}_s + k_{es}E_s, \tag{43}$$

where k_{es} is a diagonal matrix consisting positive constant elements, $\frac{d}{dt}W_3$ can be written by Equation (44):

$$\tfrac{d}{dt}W_3 = -\mathrm{k}_{es}\mathrm{E}_s^T \mathrm{E}_s \le 0. \tag{44}$$

Hence, the time derivative of the chosen Lyapunov function is negative definite, indicating asymptotic stability of the power control system.

4.2.2. Compensation of unbalanced load current

In Figure 1, it is considered that a combination of both balanced and unbalanced loads is connected to the Grid-following unit's PC buses. In addition to generate pre-specified powers, the control objective is to compensate the effect of an unbalanced load by injecting required NSCCs by the corresponding Grid-following unit. For this purpose, the instantaneous power reference of Grid-following unit is determined as Equation (45):

$$S^{ref} = S^{pre-set} + \frac{3}{2} E_f I_L^n \tag{45}$$

where, I_L^n is the NSCCs of local load of Grid-following unit. In order to regulate the active/reactive of Grid-following unit and to generate the NSCCs of the local load, the obtained power reference is robustly tracked by the proposed direct power controller.

5. Simulation Results

To assess the effectiveness of the proposed control strategy, the MG depicted in Figure 1 is simulated using the MATLAB/Simulink software environment. The system parameters can be found in Table 1. In the studied MG, the Grid-forming (DG_1) unit utilizes the proposed voltage controller, while the Grid-following (DG_2) unit employs the proposed power controller. The study includes four simulation cases, each detailed in the subsequent subsections. The case studies provide insights into the MG performance under various scenarios, including parametric uncertainties, the black start process, energization with unbalanced loads, and the accidental outage of Grid-following units. It's important to highlight that across all case studies, the parameters and topology of the controllers remain consistent.

5.1. Microgrid Black-Start

The objective of this case study is twofold: 1) MG Black-Start Capability: It aims to showcase the MG's ability to black-start, which refers to the process of restoring power to the system after a complete shutdown. 2) Robustness of Proposed Control Strategy: The study evaluates the robustness of the proposed control strategy in the face of parametric uncertainties within the MG. In studies, the Grid-forming unit is black-started with $V_f^{ref} = 0$, while the power reference of Grid-following unit is set to $P_2^{ref} = 0$ and $Q_2^{ref} = 0$. Subsequently, V_f^{ref} is increased to 1 p.u. with an exponentially trajectory. In this study, the robust performance of the proposed controllers is assessed under parametric uncertainties. Specifically, a 20% step-mismatch is introduced in the filter resistance starting from $t = 0.3$ s.

At $t = 0.4$ s and $t = 0.8$ s, the active/reactive power components of the reference signal of DG2, are exponentially increased to 0.4 p.u. and 0.3 p.u., respectively, with 0.005 s time-constant. The response of MG to explained events is depicted in Figure 3. The voltage magnitude of DG1 is indicated in Figure 3(a). This quantity can be obtained by Equation (46):

$$V = \sqrt{(V_d)^2 + (V_q)^2} \tag{46}$$

According to Figure 3(a), the filter voltage exhibits a stable and rapid response as it closely follows its reference command. Notably, this behavior demonstrates strong robustness even in the presence of parametric uncertainties and during the black-start process of the Grid-forming unit. The active/reactive power components of DG2 and DG1 are depicted in Figure 3(b) and (c). According to Figure 3(b), the active/reactive powers of the Grid-following unit closely track their respective reference signals. Notably, there are no observable transients or inter-channel interactions. In Figure 3(d), the voltage magnitude at the point of common coupling (PCC) can be observed. Additionally, Figure 3(e) and Figure 3(f) provide zoomed views of the voltage waveform at the PCC for periods around t = 0.4 s and t = 0.8 s, respectively. Based on the information provided, the transients of the PCC voltage are practically insignificant. This case study serves as a demonstration of the robust performance of the proposed control strategy. Despite uncertainties in system parameters and the black-start process of the Grid-forming unit, the strategy effectively tracks reference commands and maintains system stability. Additionally, it validates the MG's black-start capability under the presented control method.

5.2. Unbalanced Load Energization

5.2.1. Energization of Unbalanced Load1

In this case study, the focus is on demonstrating the robust performance of the proposed voltage controller under unbalanced load conditions. Despite the challenges posed by varying loads, the controller aims to maintain stability and effectively regulate the system. In this case study, we consider the following scenario: 1 (The MG system initially operates under the conditions described in Subsection 5.1. 2) At $t = 1.7$ s, an unbalanced load is connected to the low-voltage side of feeder F_1. In this case study, the unbalanced load connected to the MG system consists of a series RL circuit between phase-b and phase-c. Specifically: the load resistance is 3.6Ω and the load inductance is $8.6 mH$.

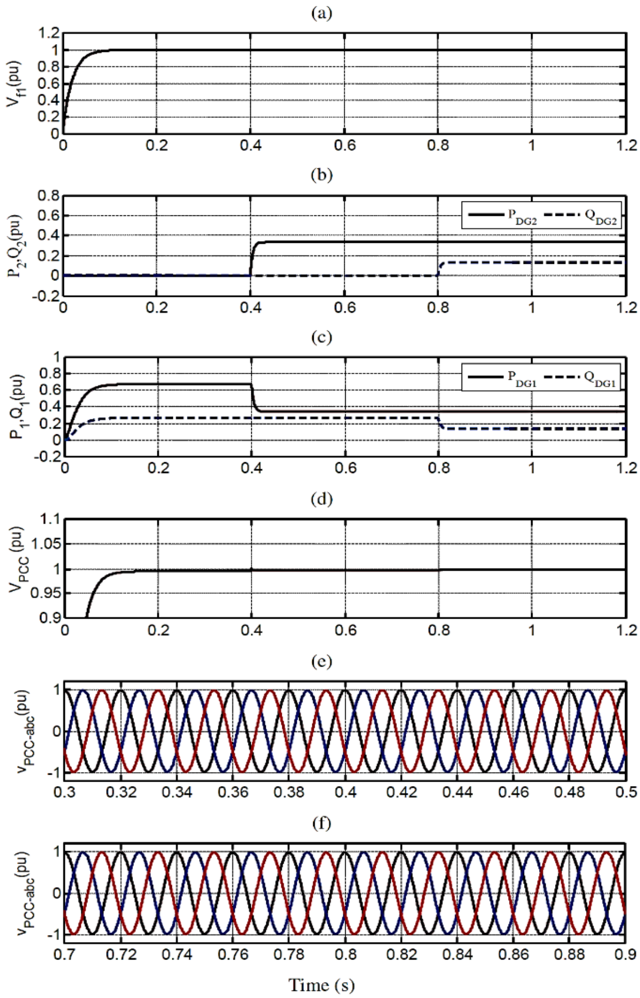

Figure 3. Black-start of Grid-forming unit and energization of a Grid-following unit: (a) magnitude of output voltage of DG1, (b) and (c) active/reactive power components of DG2 and DG1, (d) PCC voltage magnitude, and (e) and (f) instantaneous PCC voltage around $t=0.4$ s and $t=0.8$ s.

Figure 4(a)-(g) indicated the instantaneous current of load, the load current magnitude, output power components of DG1 and DG2, the voltage magnitude of the PCC and filter, and the PCC bus's instantaneous voltage, in a time-period around $t=1.7$ s; and depicts the dynamic response of MG to energization of the explained unbalanced load. As shown in Figure 4(a) and (b), when $Load_1$ becomes unbalanced, a notable NSCC appears in the load current. This results in an increase in the current unbalance factor (CUF)—the ratio of NS to PS components—rising from zero to approximately 33.3%. As depicted in Figure 4(b)-(d), the NSCC of the load current becomes evident through double-frequency oscillations (DFOs) observed in both the magnitude of the load current and the instantaneous active/reactive power components of the Grid-forming unit. As depicted in Figure 4(c) and 4(d), even with the unbalanced load energization, the instantaneous active/reactive power components of the Grid-following unit exhibit robust tracking of their reference values. Notably, there are no observable transients or double-frequency oscillations (DFOs) in these components. Figure 4(e), (f) and (g) provide confirmation that even under unbalanced load conditions, the proposed voltage controller effectively and robustly regulates the voltage waveform of the MG. In this case, the voltage unbalance factor (VUF)—which represents the ratio of the NS to PS components of the filter and PCC voltage—is 0.08% and 0.19%, respectively. These values fall well within the IEEE Standards requirement for voltage imbalance, which specifies a limit of below 2% for sensitive equipment. This case study serves as verification of the stability and robustness of the proposed voltage controller under unbalanced load conditions and in the presence of parameter uncertainties.

5.2.2. Energization of Unbalanced Load2

In this case study, the purpose is to assess the effectiveness of the presented power controller against load unbalance. In this case study, the MG initially operates under the same conditions explained in Subsection 5.1. In this case, an unbalanced load is energized through the low-voltage feeder of F_2 at $t=1.7$ s. The unbalanced load is composed of a resistor and an inductance connected in series with parameters of 3.6Ω and 8.6 mH, connected between phase-b and phase-c.

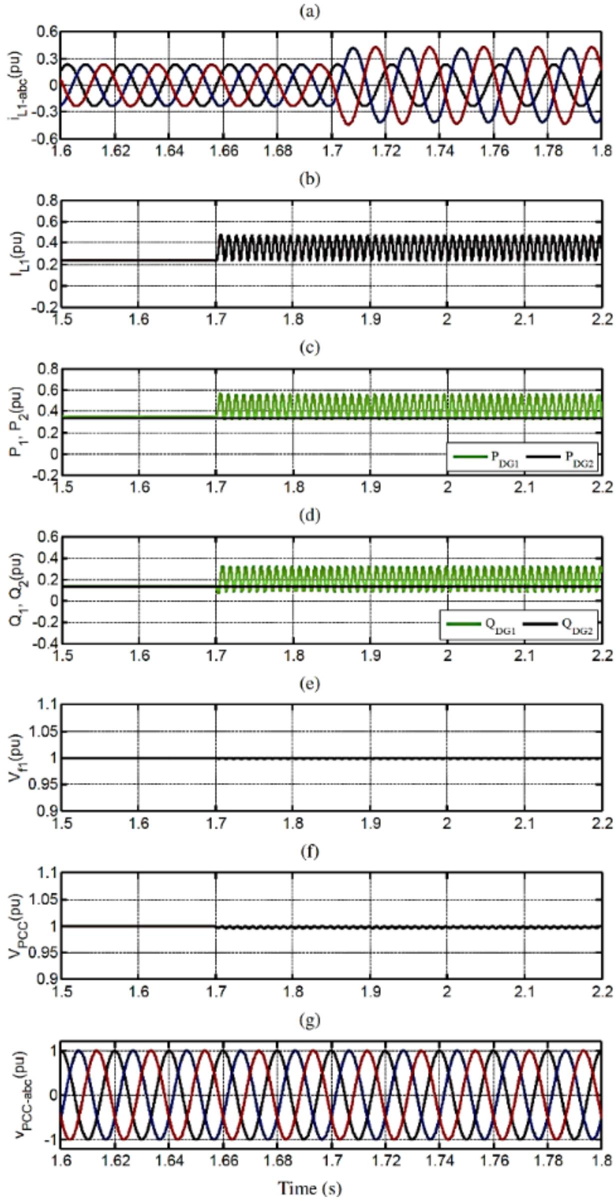

Figure 4. Energization of unbalanced Load1: (a) instantaneous load current, (b) load current amplitude, (c) active power component of DG1 and DG2, (d) reactive power component of DG1 and DG2, (e) and (f) amplitude of the PC1 and PCC voltage, and (g) instantaneous voltage of PCC bus.

In Figure 5, the system's response following the connection of the described unbalanced load can be observed. The time period of interest is about t = 1.7 s. Figure 5(a)-(b) indicate the load current in instantaneous form as well as magnitude form. As shown in Figure 5(a), since the Load2 becomes unbalanced, the load current is imposed with a significant NS component, such that an increase of about 33.3% has occurred in the load current CUF index. When analyzing the load current, the NSCC becomes evident through DFOs in the detected amplitude of the load current, as indicated in Figure 5(b). These oscillations are a result of the unbalanced load conditions that discussed earlier.

In Figure 5(c)-(d) the active/reactive power of both DG units are shown. From these plots, it can be observed that the average active and reactive power values of the Grid-following unit closely follow their respective references, even when dealing with load switching and unbalanced load conditions. However, under unbalanced load conditions, the instantaneous values of the active/reactive powers of Grid-following unit are influenced by DFOs. The DFOs related to DG2 is directly affected by NSCC of the load. The sudden variations observed in the average powers of Grid-forming unit are a result of step demand variation of the loads. Figure 5(e)-(g) shows the magnitude as well as the instantaneous voltage of PCC bus and filter. They indicate that when the load become unbalanced, the voltage waveform throughout the system is robustly regulated by the presented control structure. The VUF of both the filter and PCC voltage in this case are less than 0.01%. This case study demonstrates that subject to unbalanced load conditions, the control system designed in this paper is stable and robust.

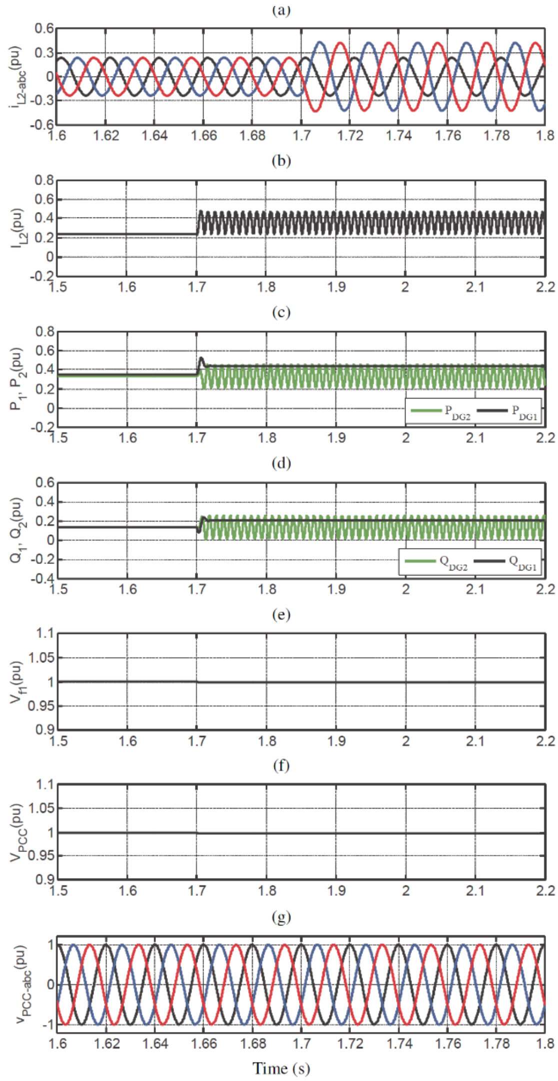

Figure 5. Energization of unbalanced Load2: (a) instantaneous load current, (b) load current amplitude, (c) active power component of DG1 and DG2, (d) reactive power component of DG1 and DG2, (e) and (f) amplitude of the PC1 and PCC voltage, and (g) instantaneous voltage of PCC bus.

5.3. Unexpected disconnection of Grid-following Unit, under unbalance conditions

The purpose of this case study is to verify whether the proposed voltage control structure can ensure the stability of the MG following an unexpected disconnection of the Grid-following unit. This outage is considered a large-signal disturbance. The only condition for stability is that the demand of the MG must can be met by the Grid-forming unit. Before the Grid-following unit disconnection, the MG system operates according to the conditions outlined in Subsection 5.2.2. At t = 2 s, the Grid-following unit is disconnected from the MG and the loads of feeder F2 are supplied by the Grid-forming unit. Figure 6(a)-(g) shows the load current magnitude, the instantaneous active/reactive power of the both DG units, a zoomed view of P_{DG1} and Q_{DG1}, amplitude of the filter and PCC voltage, and instantaneous value of PCC voltage. Considering these plots, it can be seen that after outage of Grid-following unit, the power generated by the Grid-forming unit is adaptively adjusted so that the absence of generation at PC2 is offset. In addition, despite the mismatched filter resistance and accidental outage of Grid-following unit, even under non-local unbalanced load condition, the proposed voltage controller robustly regulates the voltage waveform of MG with a reasonable transient, as indicated in Figure 6(e)-(g).

6. Conclusions

In this paper, a robust control structure is presented for islanded operation of a MG comprises several buses fed by multiple inverter-based DG units. In this proposed control strategy, the Grid-forming/Grid-following structure is utilized. Specifically, an adaptive Backstepping control method is employed to ensure that the voltage magnitude and frequency of the Grid-forming unit closely follow predefined trajectories. This approach aims to enhance stability and reliability in the operation of the multi-bus microgrid. In this paper, an adaptive direct power controller using the IOFL control method is also presented that its purpose is to regulate the active/reactive power supplied by the Grid-following units. The effectiveness of the proposed control scheme is demonstrated through various simulation case studies conducted in the MATLAB/Simulink software. These simulations confirm the robust and stable performance of the control scheme, even in the presence of MG parameter uncertainties, black-start scenarios, unbalanced load energization, and sudden accidental outages of Grid-following units under unbalanced load conditions. The important results of the article are summarized as follows:

- The proposed control scheme is designed based on local measurements and is operated independent from the MG loads characteristics.
- The lumped uncertainties respectively effects on dynamics of voltage as well as power of Grid-forming and Grid-following units, containing disturbances and parameters variations, are compensated by an adaptive estimation method.
- These adaptive terms enhance the system's robustness against measurement errors and modeling inaccuracies.

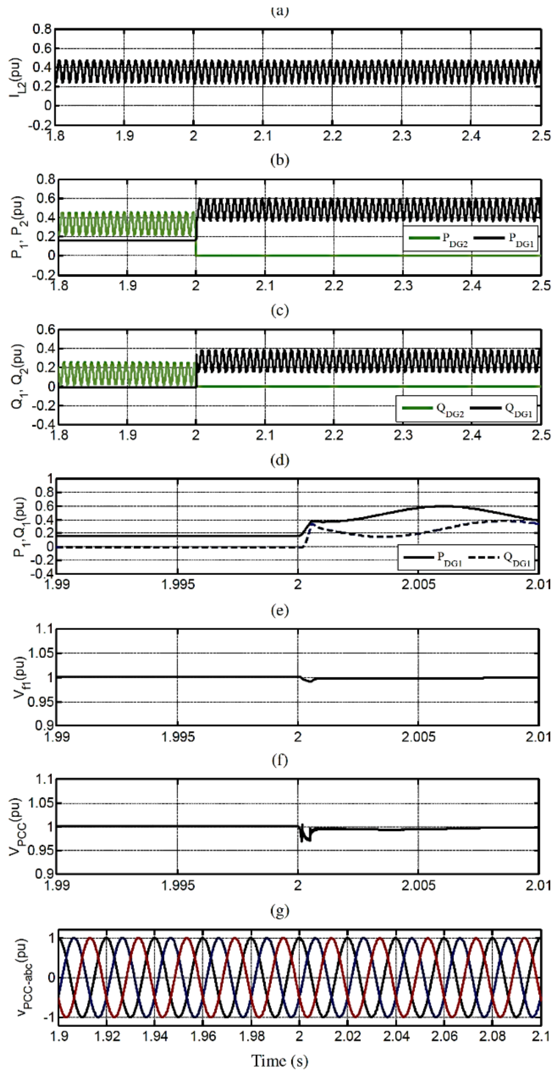

Figure 6. Accident outage of Grid-following unit: (a) load current amplitude, (b) active power component of DG1 and DG2, (c) reactive power component of DG1 and DG2, zoomed view of (d) P_{DG1} and Q_{DG1}, (e) amplitude of the PC1 voltage, (f) amplitude of PCC bus voltage, and (g) instantaneous voltage of PCC bus.

References

[1] M. M. Rezaei, and J. Soltani, "Sliding Mode Control of a Grid-Connected Distributed Generation Unit Under Unbalanced Voltage Conditions," *Automatika*, vol. 57, no. 1, pp. 89–98, 2016.

[2] H. Eshghi, J. Soltani, M. M. Rezaei, and S. Shojaeian, "A Robust Control Strategy for a Single-phase Grid-connected Multibus Microgrid Based on Adaptive Sliding Mode Control and Dynamic Phasor Concept," *International Transactions on Electrical Energy Systems*, vol. 31, no. 8, 2021.

[3] M. Sakamoto, and H. Haga, "Control Method for Universal Smart Power Module Considering Wireless Communication," *IEEJ Journal of Industry Applications*, vol. 12, no. 2, pp. 204–214, 2023.

[4] S. Abdalfatah, E. E. El-kholy, and H. Awad, "Power-Sharing in Microgrids by Adaptive Virtual Impedance and Fuzzy Logic," *Engineering Research Journal*, vol. 179, no. 0, pp. 68–74, 2023.

[5] M. K. Behera, and L. C. Saikia, "A Novel Spontaneous Control for Autonomous Microgrid VSC System Using BPF Droop and Improved Hysteresis Band Control Scheme,"

Electric Power Systems Research, vol. 220, 109262, 2023.
[6] M. M. Rezaei, and J. Soltani, "A Robust Control Strategy for a Grid-Connected Multi-Bus Microgrid Under Unbalanced Load Conditions," *International Journal of Electrical Power & Energy Systems*, vol. 71, pp. 68–76, 2015.
[7] M. J. Morshed, and A. Fekih, "Design of a chattering-free Integral Terminal Sliding Mode Approach for DFIG-based Wind Energy Systems," *Optimal Control Applications and Methods*, vol. 41, no. 5, pp. 1718–1734, 2020.
[8] S. Harasis, "Controllable Transient Power Sharing of Inverter-Based Droop Controlled Microgrid," *International Journal of Electrical Power & Energy Systems*, vol. 155, 109565, 2024.
[9] H. H. Goh, X. Zhang, et al., "Harmonic Virtual Impedance Control in Islanded Microgrids for Harmonic Power Sharing and Harmonic Suppression," *CSEE Journal of Power and Energy Systems*, 2024.
[10] T. John, and U. Khan, "A Control Architecture for Regulating Voltage and Power Flows in a Networked Microgrid System," *International Transactions on Electrical Energy Systems*, vol. 2024, pp. 1–14, 2024.
[11] E. Rokrok, F. Shavakhi Zavareh, J. Soltani, and M. R. Shakarami, "A Robust Control Strategy for Distributed Generations in Islanded Microgrids," *AUT Journal of Electrical Engineering*, vol. 52, no. 1, pp. 107-120, 2020.
[12] M. Zhang, Y. Han, et al., "Multi-Timescale Modeling and Dynamic Stability Analysis for Sustainable Microgrids: State-Of-The-Art and Perspectives," *Protection and Control of Modern Power Systems*, vol. 9, no. 3, pp. 1–35, 2024.
[13] S. Chen, Y. Sun, et al., "A First-Order PLL-Synchronized Voltage-Supporting Control Method for Parallel Inverters with Near-Zero Line Impedance," *IEEE Transactions on Power Electronics*, vol. 39, no. 8, pp. 9072–9078, 2024.
[14] X. Lin, R. Yu, J. Yu, and H. Wen, "Dual-Frames-Impedance-Based Analysis of Dynamic Phase Difference Effect on Grid-Forming Converter with Different Power Synchronization Controls," *International Journal of Electrical Power & Energy Systems*, vol. 158, 109928, 2024.
[15] L. S. Arunagiri, B. S. Rajpurohit, and A. Jain, "Control of Distribution Static Compensator with Active Damped Inductor-Capacitor-Inductor Filter Using Dual Loop $\alpha\beta$-Frame Current Controllers for Power Quality Improvement," *IET Energy Systems Integration*, vol. 5, no. 2, pp. 128–151, 2022.
[16] W. Pinthurat, B. Hredzak, G. Konstantinou, and J. Fletcher, "Techniques for Compensation of Unbalanced Conditions in LV Distribution Networks with Integrated Renewable Generation: An Overview," *Electric Power Systems Research*, vol. 214, 108932, 2023.
[17] S. A. Yahyaee, P. Sreekumar, and V. Khadkikar, "A Novel Decentralized Unbalance Load Sharing Approach for Islanded Microgrids," *2022 IEEE Industry Applications Society Annual Meeting (IAS)*, pp. 1–7, 2022.
[18] B. Sharma, P. K. Pankaj, et al., "Power Sharing in Three-Level NPC Inverter Based Three-Phase Four-Wire Islanding Microgrids with Unbalanced Loads," *IEEE Access*, vol. 11, pp. 20725–20740, 2023.
[19] M. Dehghani, A. Kavousi-Fard, T. Niknam, and O. Avatefipour, "A Robust Voltage and Current Controller of Parallel Inverters in Smart Island: A Novel Approach," *Energy*, vol. 214, 118879, 2021.
[20] M. J. Hossain, H. R. Pota, M. A. Mahmud, and M. Aldeen, "Robust Control for Power Sharing in Microgrids with Low-Inertia Wind and PV Generators," *IEEE Transactions on Sustainable Energy*, vol. 6, no. 3, pp. 1067–1077, 2015.
[21] B. E. Sedhom, M. M. El-Saadawi, M. A. Elhosseini, M. A. Saeed, and E. E. Abd-Raboh, "A Harmony Search-Based H-Infinity Control Method for Islanded Microgrid," *ISA Transactions*, vol. 99, pp. 252–269, 2020.
[22] M. Shafiee-Rad, Q. Shafiee, M. S. Sadabadi, and M. R. Jahed-Motlagh, "Decentralized Voltage Stabilization and Robust Performance Satisfaction of Islanded Inverter-Interfaced Microgrids," *IEEE Systems Journal*, vol. 15, no. 2, pp. 1893–1904, 2021.
[23] M. Armin, M. Rahman, et al., "Robust Extended H_∞ Control Strategy Using Linear Matrix Inequality Approach for Islanded Microgrid," *IEEE Access*, vol. 8, pp. 135883–135896, 2020.
[24] M. Hamzeh, H. Karimi, and H. Mokhtari, "A New Control Strategy for a Multi-Bus MV Microgrid Under Unbalanced Conditions," *IEEE Transactions on Power Systems*, vol. 27, no. 4, pp. 2225–2232, 2012.
[25] M. M. Rezaei, and J. Soltani, "Robust Control of an Islanded Multi-bus Microgrid Based on Input–output Feedback Linearisation and Sliding Mode Control," *IET Generation, Transmission & Distribution*, vol. 9, no. 15, pp. 2447–2454, 2015.
[26] A. Sotoudeh, and M. Rezaei, "Robust Control of Isolated SCIG-Based WECS Feeding Constant Power Load Using Adaptive Backstepping and Fractional Order PI Methods," *International Journal of Dynamics and Control*, vol. 12, no. 2, pp. 452–462, 2023.
[27] J. J. E. Slotine, and W. Li, "Applied Nonlinear Control," *Englewood Cliffs*, vol. 199, no. 1, p. 705, 1991.
[28] J. A. Suul, A. Luna, P. Rodríguez, and T. Undeland, "Virtual-Flux-Based Voltage-Sensor-Less Power Control for Unbalanced Grid Conditions," *IEEE Transactions on Power Electronics*, vol. 27, no. 9, pp. 4071–4087, 2012.
[29] IEEE P 1159 Working Group, "Recommended Practice for Monitoring Electric Power Quality," *Technical Report*, Draft 5, 1994.

Declaration of competing interest

The authors declare that they have no known competing financial interests or personal relationships that could have appeared to influence the work reported in this paper. The ethical issues, including plagiarism, informed consent, misconduct, data fabrication and/or falsification, double publication and/or submission, redundancy, have been completely observed by the authors.

Bibliography

Mohammad Mahdi Rezaei received the M.Sc. degree in electrical engineering from Amirkabir University of Technology (Tehran Polytechnic), Tehran, Iran, in 2007, and the Ph.D. degree in electrical engineering from the Science and Research Branch, Islamic Azad University, Tehran, Iran, in 2015. He is currently an Associated Professor in the Department of Electrical and Computer Engineering, Khomeinishahr Branch, Islamic Azad University, Isfahan, Iran. His main areas of research are control of microgrids, distributed generations, and design, optimization and implementation of electrical drives.

Email: mm.rezaei@iaukhsh.ac.ir
ORCID: 0000-0002-8569-3170

Contribution Statement: Conceptualization, Funding acquisition, Investigation, Project administration, Resources, Supervision, Validation, Roles/Writing - original draft, Writing-review & editing.